Learning Fair Representations via Rate-Distortion Maximization

Somnath Basu Roy Chowdhury and **Snigdha Chaturvedi**

UNC Chapel Hill, USA

{somnath, snigdha}@cs.unc.edu

Abstract

Text representations learned by machine learning models often encode undesirable demographic information of the user. Predictive models based on these representations can rely on such information, resulting in biased decisions. We present a novel debiasing technique, **Fa**irness-aware **R**ate **M**aximization (FaRM), that removes protected information by making representations of instances belonging to the same protected attribute class uncorrelated, using the rate-distortion function. FaRM is able to debias representations with or without a target task at hand. FaRM can also be adapted to remove information about multiple protected attributes simultaneously. Empirical evaluations show that FaRM achieves state-of-the-art performance on several datasets, and learned representations leak significantly less protected attribute information against an attack by a non-linear probing network.

1 Introduction

Democratization of machine learning has led to deployment of predictive models for critical applications like credit approval (Ghailan et al., 2016) and college application reviewing (Basu et al., 2019). Therefore, it is important to ensure that decisions made by these models are *fair* towards different demographic groups (Mehrabi et al., 2021). Fairness can be achieved by ensuring that the demographic information does not get encoded in the representations used by these models (Blodgett et al., 2016; Elazar and Goldberg, 2018; Elazar et al., 2021).

However, controlling demographic information encoded in a model's representations is a challenging task for textual data. This is because natural language text is highly indicative of an author's demographic attributes even when it is not explicitly mentioned (Koppel et al., 2002; Burger et al., 2011; Nguyen et al., 2013; Verhoeven and Daelemans, 2014; Weren et al., 2014; Rangel et al., 2016; Verhoeven et al., 2016; Blodgett et al., 2016).

In this work, we *debias* information about a protected attribute (e.g., gender, race) from textual data representations. Previous debiasing methods (Bolukbasi et al., 2016; Ravfogel et al., 2020) project representations in a subspace that does not reveal protected attribute information. These methods are only able to guard protected attributes against an attack by a linear function (Ravfogel et al., 2020). Other methods (Xie et al., 2017; Basu Roy Chowdhury et al., 2021) adversarially remove protected information while retaining information about a target attribute. However, they are difficult to train (Elazar and Goldberg, 2018) and require a target task at hand.

We present a novel debiasing technique, **Fa**irness-aware **R**ate **M**aximization (FaRM), that removes demographic information by controlling the *rate-distortion* function of the learned representations. Intuitively, in order to remove information about a protected attribute from a set of representations, we want the representations from the same protected attribute class to be uncorrelated to each other. We achieve this by maximizing the number of bits (rate-distortion) required to encode representations with the same protected attribute. Figure 1 illustrates the process. The representations are shown as points in a two-dimensional feature space, color-coded according to their protected attribute class. FaRM learns a function $\phi(x)$ such that representations of the same protected class become uncorrelated and similar to other representations, thereby making it difficult to extract the information about the protected attribute from the learned representations.

We perform rate-distortion maximization based debiasing in the following setups: (a) *unconstrained debiasing*—we remove information about a protected attribute **g** while retaining remaining information as much as possible (e.g., debiasing gender information from word
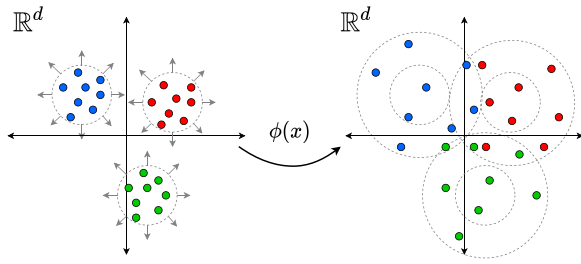
1159

Figure 1: Illustration of unconstrained debiasing using FaRM. Representations are color-coded (in blue, red and green) according to their protected attribute class. Before debiasing (left), representations within each class are similar to each other (intra-class information content is low). Debiasing enforces the within class representations to be uncorrelated by increasing their information content.

embeddings), and (b) *constrained debiasing*—we retain information about a target attribute **y** while removing information pertaining to **g** (e.g., removing racial information from representations during text classification). In the unconstrained setup, debiased representations can be used for different downstream tasks, whereas for constrained debiasing the user is interested only in the target task. For unconstrained debiasing, we evaluate FaRM for removing gender information from word embeddings and demographic information from text representations that can then be used for a downstream NLP task (we show their utility for biography and sentiment classification in our experiments). Our empirical evaluations show that representations learned using FaRM in an unconstrained setup leak significantly less protected attribute information compared to prior approaches against an attack by a non-linear probing network.

For constrained debiasing, FaRM achieves state-of-the-art debiasing performance on 3 datasets, and representations are able to guard protected attribute information significantly better than previous approaches. We also perform experiments to show that FaRM is able to remove multiple protected attributes simultaneously while guarding against intersectional group biases (Subramanian et al., 2021). To summarize, our main contributions are:

- We present **Fa**irness-aware **R**ate **M**aximization (FaRM) for debiasing of textual data representations in unconstrained and constrained setups, by controlling their rate-distortion functions.

- We empirically show FaRM leaks significantly less protected information against a non-linear probing attack, outperforming prior approaches.

- We present two variations of FaRM for debiasing multiple protected attributes simultaneously, which is also effective against an attack for intersectional group biases.

2 Related Work

Removing sensitive attributes from data representations for fair classification was initially introduced as an optimization task (Zemel et al., 2013). Subsequent works have used adversarial frameworks (Goodfellow et al., 2014) for this task (Zhang et al., 2018; Li et al., 2018; Xie et al., 2017; Elazar and Goldberg, 2018; Basu Roy Chowdhury et al., 2021). However, adversarial networks are difficult to train (Elazar and Goldberg, 2018) and cannot function without a target task at hand.

Unconstrained debiasing frameworks focus on removing a protected attribute from representations, without relying on a target task. Bolukbasi et al. (2016) demonstrated that GloVe embeddings encode gender information, and proposed an unconstrained debiasing framework for identifying gender direction and neutralizing vectors along that direction. Building on this approach, Ravfogel et al. (2020) proposed INLP, a robust framework to debias representations by iteratively identifying protected attribute subspaces and projecting representations onto the corresponding nullspaces. However, these approaches fail to guard protected information against an attack by a non-linear probing network. Dev et al. (2021) showcased that nullspace projection approaches can be extended for debiasing in a constrained setup as well.

In contrast to prior works, we present a novel debiasing framework based on the principle of rate-distortion maximization. Coding rate maximization was introduced as an objective function by Ma et al. (2007) for image segmentation. It has also been used in explaining feature selection by deep networks (Macdonald et al., 2019). Recently, Yu et al. (2020) proposed maximal coding rate (MCR^2) based on rate-distortion theory, a representation-level objective function that can serve as an alternative to empirical risk minimization methods. Our work is similar to MCR^2 as we learn representations using a rate-distortion

framework, but instead of tuning representations for classification we remove protected attribute information from them.

3 Preliminaries

Our framework performs debiasing by making representations of the same protected attribute class uncorrelated. To achieve this, we leverage a principled objective function called rate-distortion, to measure the compactness of a set of representations. In this section, we introduce the fundamentals of rate-distortion theory.[1]

Rate-Distortion. In lossy data compression (Cover, 1999), the compactness of a random distribution is measured by the minimal number of binary bits required to encode it. A lossy coding scheme encodes a finite set of vectors $Z = \{z_1, \ldots, z_n\} \in \mathbb{R}^{n \times d}$ from a distribution $P(Z)$, such that the decoded vectors $\{\hat{z}_i\}_{i=1}^n$ can be recovered up to a precision ϵ^2. The *rate-distortion* function $R(Z, \epsilon)$ measures the minimal number of bits per vector required to encode the sequence Z.

In case the vectors $\{z_i\}_{i=1}^n$ are i.i.d. samples from a zero-mean multi-dimensional Gaussian distribution $\mathcal{N}(0, \Sigma)$, the optimal rate-distortion function is given as:

$$R(Z, \epsilon) = \frac{1}{2} \log_2 \det \left(I + \frac{d}{n\epsilon^2} Z Z^T \right) \quad (1)$$

where $\frac{1}{n} Z Z^T = \hat{\Sigma}$ is the estimate of covariance matrix Σ for the Gaussian distribution. As the eigenvalues of the matrices $Z Z^T$ and $Z^T Z$ are equal, the rate-distortion function $R(Z, \epsilon)$ is the same for both of them (Ma et al., 2007). In most setups $d \ll n$, therefore, we use $Z^T Z$ for efficiently computing $R(Z, \epsilon)$.

In rate-distortion theory, we need $nR(Z, \epsilon)$ bits to encode n vectors of Z. The optimal codebook also depends on data dimension (d) and requires $dR(Z, \epsilon)$ bits to encode. Therefore, a total of $(n + d)R(Z, \epsilon)$ is bits required to encode the sequence Z. Ma et al. (2007) showed that this provides a tight bound even in cases where the underlying distribution $P(Z)$ is degenerate. This enables the use of this loss function for real-world data, where the underlying distribution may not be well defined.

In general, a set of compact vectors (low information content) would require a small number of bits to encode, which would correspond to a small value of $R(Z, \epsilon)$ and vice versa.

Rate Distortion for a Mixed Distribution. In general, the set of vectors Z can be from a mixture distribution (e.g., feature representations for multi-class data). The rate-distortion function can be computed by splitting the data into multiple subsets: $Z = Z^1 \cup Z^2 \ldots \cup Z^k$, based on their distribution. For each subset, we can compute the $R(Z^i, \epsilon)$ (Equation 1). To facilitate the computation, we define a membership matrix $\Pi = \{\Pi_j\}_{j=1}^k$ as a set of k matrices to encode membership information in each subset Z^j. The membership matrix Π_j for each subset is a diagonal matrix defined as:

$$\Pi_j = \text{diag}(\pi_{1j}, \pi_{2j}, \ldots, \pi_{nj}) \in \mathbb{R}^{n \times n} \quad (2)$$

where $\pi_{ij} \in [0, 1]$ denotes the probability of a vector z_i belonging to the j-th subset and n is the number of vectors in the sequence Z. The matrices satisfy the constraints: $\sum_j \pi_{ij} = 1$, $\sum_j \Pi_j = I_{n \times n}$, $\Pi_j \succeq 0$. The expected number of vectors in the j-th subset Z^j is $\text{tr}(\Pi_j)$ and the corresponding covariance matrix: $\frac{1}{\text{tr}(\Pi_j)} Z \Pi_j Z^T$. The overall rate-distortion function is given as:

$$R^c(Z, \epsilon | \Pi) =$$
$$\sum_{j=1}^k \frac{\text{tr}(\Pi_j)}{2n} \log_2 \det \left(I + \frac{d}{\text{tr}(\Pi_j)\epsilon^2} Z \Pi_j Z^T \right)$$

For multi-class data, where a vector z_i can only be a member of a single class, we restrict $\pi_{ij} = \{0, 1\}$, and therefore the covariance matrix for the j-th subset is $Z^j Z^{j^T}$. In general, if the representations within each subset Z^j are similar to each other, they will have low intra-class variance, and it would correspond to a small $R^c(Z, \epsilon | \Pi)$ and vice versa.

4 Fairness-Aware Rate Maximization

In this section, we describe FaRM to debias representations in unconstrained and constrained setups.

4.1 Unconstrained Debiasing using FaRM

In this setup, we aim to remove information about a protected attribute **g** from data representations

---

Algorithm 1 Unconstrained Debiasing Routine

1: **Input**: (X, G) input data set with protected attribute labels. Number of training epochs N.
2: **for** $i = 1, \ldots, N$ **do**
3:      $Z = \text{LayerNorm}(\phi(X))$
4:      $\Pi^{\mathbf{g}} = \text{ConstructMatrix}(G)$ ▷ retrieve membership matrix using G
5:      Update ϕ using gradients $\nabla_{\phi} J_u(Z, \Pi^{\mathbf{g}})$
6: **end for**
7: $Z_{\text{debiased}} = \phi(X)$ ▷ debiased representations
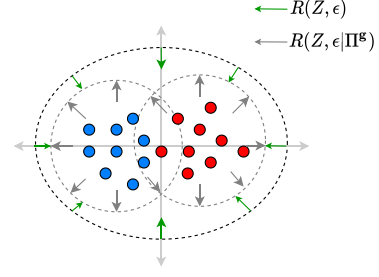8: **return** ϕ ▷ debiasing network

---

Figure 2: Visualization for regularization loss in J_c for constrained debiasing. The **red** and **blue** circles represent 2D representations from two different protected class. The **gray** arrows are induced by $R^c(Z, \epsilon | \Pi^{\mathbf{g}})$ term and the **green** ones are induced by $R(Z, \epsilon)$ term.

X while retaining the remaining information. To achieve this, the debiased representations Z should have the following properties:

(a) *Intra-class Incoherence*: Representations belonging to the same protected attribute class should be highly uncorrelated. This would make it difficult for a classifier to extract any information about **g** from the representations.

(b) *Maximal Informativeness*: Representations should be maximally informative about the remaining information.

Assuming that there are k protected attribute classes, we can write $Z = Z^1 \cup \ldots \cup Z^k$. To achieve (a), we need to ensure that the representations in a subset Z^j belonging to the same protected class are dissimilar and have large intra-class variance. An increased intra-class variance would correspond to an increase in the number of bits to encode samples within each class and the rate-distortion function $R^c(Z, \epsilon | \Pi^{\mathbf{g}})$ would be *large*. For (b), we want the representations Z to retain maximal possible information from the input X. Increasing information content in Z, would require a larger number of bits to encode it. This means that the rate-distortion $R(Z, \epsilon)$ should also be *large*.

FaRM achieves (a) and (b) simultaneously by *maximizing* the following objective function:

$$J_u(Z, \Pi^{\mathbf{g}}) = R^c(Z, \epsilon | \Pi^{\mathbf{g}}) + R(Z, \epsilon) \quad (3)$$

where the membership matrix $\Pi^{\mathbf{g}}$, is constructed using the protected attribute **g** (see Equation 2).

The unconstrained debiasing routine is described in Algorithm 1. We use a deep neural network ϕ as our feature map to obtain debiased representations $z = \phi(x)$. The objective function J_u is sensitive to the scale of the representations. Therefore, we normalize the Frobenius norm of the representations to ensure individual input samples have an equal impact on the loss. We use layer normalization (Ba et al., 2016) to ensure that all representations have the same magnitude and lie on a sphere $z_i \in \mathbb{S}^{d-1}(r)$ of radius r. The feature encoder ϕ is updated using gradients from the objective function J_u. The debiased representations are retrieved by feeding input data X through the trained network ϕ. An illustration of the debiasing process in the unconstrained setup is shown in Figure 1.

4.2 Constrained Debiasing using FaRM

In this setup, we aim to remove information about a protected attribute **g** from data representations X while retaining information about a specific target attribute **y**. The learned representations should have the following properties:

(a) *Target-Class Informativeness*: Representations should be maximally informative about the target task attribute **y**.

(b) *Inter-class Coherence*: Representations from different protected attribute classes should be *similar* to each other. This would make it difficult to extract information about **g** from Z.

Our constrained debiasing setup is shown in Figure 3, where representations are retrieved from
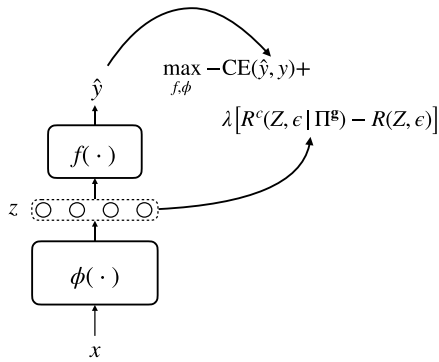
Figure 3: Constrained debiasing setup using FaRM. Representation z retrieved from the feature map ϕ is used to predict the target label and control the rate-distortion objective function.

a feature map ϕ followed by a target task classifier f. In this setup, we achieve (a) by training f to predict the target class $\hat{y} = f(z)$ and minimize the cross-entropy loss $\text{CE}(\hat{y}, y)$, where y is the ground-truth target label. For (b), we need to ensure that representations from different protected classes are similar and overlap in the representation space. This is achieved by *maximizing* the rate $R^c(Z, \epsilon | \Pi^{\mathbf{g}})$ while *minimizing* $R(Z, \epsilon)$. Maximizing $R^c(Z, \epsilon | \Pi^{\mathbf{g}})$ ensures samples in the same protected class are dissimilar and have large intra-class variance. However, simply increasing intra-class variance does not guarantee the overlap of different protected class representations—as the overall feature space can expand and representations can still be discriminative w.r.t. $\mathbf{g}$. Therefore, we also minimize $R(Z, \epsilon)$ ensuring a lower number of bits are required to encode all representations Z, thereby making the representation space compact. This process is illustrated visually in Figure 2. The **blue** and **red** circles correspond to representations from two protected classes. The **gray** arrows are induced by the term $R^c(Z, \epsilon | \Pi^{\mathbf{g}})$ that encourages the representations to be dissimilar to samples in the same protected class. The **green** arrows induced by $R(Z, \epsilon)$ try to make the representation space more compact. To achieve this objective, FaRM adds a rate-distortion based regularization constraint to the target classification loss. Overall, FaRM achieves (a) and (b) simultaneously by *maximizing* the following objective function:

$$
\begin{aligned}
J_c(Z, Y, \Pi^{\mathbf{g}}) = &-\text{CE}(\hat{y}, y) \\
&+ \lambda \big[R^c(Z, \epsilon | \Pi^{\mathbf{g}}) - R(Z, \epsilon) \big]
\end{aligned} \tag{4}
$$

where $\hat{y}$ is the target prediction label, y is the ground-truth label and λ is a hyperparameter.[2] We select the hyperparameters using grid search and discuss the hyperparameter sensitivity of FaRM in Section 8. We follow a similar routine to obtain debiased representations in the constrained setup as shown in Algorithm 1.

5 Experimental Setup

In this section, we discuss the datasets, experimental setup, and metrics used for evaluating FaRM. The implementation of FaRM is publicly available at `https://github.com/brcsomnath/FaRM`.

5.1 Datasets

We evaluate FaRM using several datasets. Among these, the DIAL and Biographies datasets are used for evaluating both constrained and unconstrained debiasing. PAN16 and GloVe embeddings are used only for constrained and unconstrained debiasing, respectively. We use the same train-test split as prior works for all datasets.

(a) **DIAL** (Blodgett et al., 2016) is a Twitter-based sentiment classification dataset. Each tweet is associated with sentiment and mention labels (treated as the *target attribute* in constrained evaluation) and ''race'' information (*protected attribute*) of the author. The sentiment labels are ''happy'' or ''sad'' and the race categories are ''African-American English'' (AAE) or ''Standard American English'' (SAE).

(b) **Biography classification** dataset (De-Arteaga et al., 2019) contains biographies that are associated with a profession (*target attribute*) and gender label (*protected attribute*). There are 28 distinct profession categories and 2 gender classes.

(c) **PAN16** (Rangel et al., 2016) is also a Tweet-classification dataset where each Tweet is annotated with the author's age and gender information, both of which are binary protected attributes. The target task is mention detection.

(d) **GloVe embeddings**: We follow the setup of Ravfogel et al. (2020) to debias the most common 150,000 GloVe word embeddings (Zhao

---

[2]Note, we cannot use the same regularization term (Equation 4) for unconstrained debiasing, as minimizing $R(Z, \epsilon)$ without the supervision of target loss $\text{CE}(\hat{y}, y)$ results in all representations converging to a compact space, thereby losing most of the information.

et al., 2018). For training, we use the 7500 most male-biased, female-biased, and neutral words (determined by the magnitude of the word vector's projection onto the gender direction, which is the largest principal component of the space of vectors formed using the difference gendered word vector pairs).

5.2 Implementation Details

We use a multi-layer neural network with ReLU non-linearity as our feature map ϕ in the unconstrained setup. This setup is optimized using stochastic gradient descent with a learning rate of 0.001 and momentum of 0.9. For constrained debiasing, we used $BERT_{base}$ as ϕ, and a 2-layer neural network as f. Constrained setup is optimized using the AdamW (Loshchilov and Hutter, 2019) optimizer with a learning rate of 2×10^{-5}. We set $\lambda = 0.01$ for all experiments. Hyperparameters were tuned on the development set of the respective datasets. Our models were trained on a single Nvidia Quadro RTX 5000 GPU.

5.3 Probing Metrics

Following previous work (Elazar and Goldberg, 2018; Ravfogel et al., 2020; Basu Roy Chowdhury et al., 2021), we evaluate the quality of our debiasing by probing the learned representations for the protected attribute $\mathbf{g}$ and target attribute $\mathbf{y}$. In our experiments, we probe all representations using a non-linear classifier. We use an MLP Classifier from the scikit-learn library (Pedregosa et al., 2011). We report the Accuracy and Minimum Description Length (MDL) (Voita and Titov, 2020) for predicting $\mathbf{g}$ and $\mathbf{y}$. A large MDL signifies that more effort is needed by a probing network to achieve a certain performance. Hence, we expect debiased representations to have a *large* MDL for protected attribute $\mathbf{g}$ and a *small* MDL for predicting target attribute $\mathbf{y}$. Also, we expect a *high* accuracy for $\mathbf{y}$ and *low* accuracy for $\mathbf{g}$.

5.4 Group Fairness Metrics

TPR-GAP. Based on the notion of *equalized odds*, De-Arteaga et al. (2019) introduced TPR-GAP, which measures the true positive rate (TPR) difference of a classifier between two protected groups.
TPR-GAP for a target attribute label y is:

$$\text{TPR}_{\mathbf{g},y} = p(\hat{\mathbf{y}} = y | \mathbf{g} = g, \mathbf{y} = y)$$
$$\text{Gap}_{\mathbf{g},y} = \text{TPR}_{g,y} - \text{TPR}_{\bar{g},y}$$

where $\mathbf{y}$ is the target attribute, $\mathbf{g}$ is a binary protected attribute with possible values $g, \bar{g}$, and $\hat{\mathbf{y}}$ denotes the predicted target attribute. Romanov et al. (2019) proposed a single bias score for the classifier called $\text{Gap}_{\mathbf{g}}^{\text{RMS}}$, which is defined as:

$$\text{Gap}_{\mathbf{g}}^{\text{RMS}} = \sqrt{\frac{1}{|\mathcal{Y}|} \sum_{y \in \mathcal{Y}} (\text{Gap}_{\mathbf{g},y})^2} \quad (5)$$

where is $\mathcal{Y}$ is the set of target attribute labels.

Demographic Parity (DP). DP measures the difference in prediction w.r.t. to protected attribute $\mathbf{g}$.

$$\text{DP} = \sum_{y \in \mathcal{Y}} |p(\hat{\mathbf{y}} = y | \mathbf{g} = g) - p(\hat{\mathbf{y}} = y | \mathbf{g} = \bar{g})|$$

where $g, \bar{g}$ are possible values of the binary protected attribute $\mathbf{g}$ and $\mathcal{Y}$ is the set of possible target attribute labels.

Bickel et al. (1975) illustrated that notions of demographic parity and equalized odds can strongly differ in a real-world scenario. For representation learning, Zhao and Gordon (2019) demonstrated an inherent tradeoff between the utility and fairness of representations. TPR-GAP described above is not a good indicator of fairness if $\mathbf{y}$ and $\mathbf{g}$ are correlated, as debiasing would lead to a drop in target task performance as well. For our experiments, we compare models using both metrics for completeness. However, like prior work, in some cases we observe conflicting results due to the tradeoff.

6 Results: Unconstrained Debiasing

We evaluate FaRM for unconstrained debiasing in three different setups: word embedding debiasing, and debiasing text representations for biographies and sentiment classification. For the classification tasks, we retrieve text representations from a pre-trained encoder, debias them using FaRM (without taking the target task into account) and evaluate the debiased representations by probing for $\mathbf{y}$ and $\mathbf{g}$. In all settings, we train the feature encoder ϕ, and evaluate the retrieved representations $Z_{\text{debiased}} = \phi(X)$. All tables mention the expected trend of a metric using $\uparrow$ (higher) or $\downarrow$ (lower).

6.1 Word Embedding Debiasing

We revisit the problem of debiasing gender information from word embeddings introduced by Bolukbasi et al. (2016).

Method	Accuracy (↓)	MDL (↑)	Rank (↑)
GloVe	100.0	0.1	300
INLP	86.3	8.6	210
FaRM	**53.9**	**24.6**	**247**

Table 1: Debiasing performance on GloVe word embeddings. FaRM significantly outperforms INLP (Ravfogel et al., 2020) in guarding gender information. Best debiasing results are in **bold**.
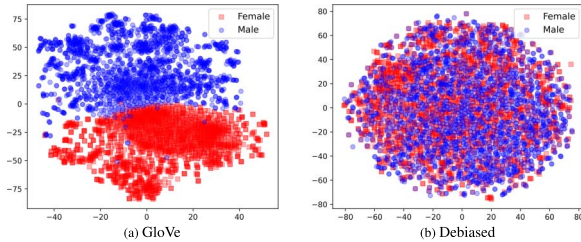

Figure 4: Projections of GloVe embeddings before (left) and after (right) debiasing. Intial female and male biased representations are shown in **red** and **blue**, respectively.

Setup. We debias gender information from GloVe embeddings using a 4-layer neural network with ReLU non-linearity as the feature map $\phi(x)$. We discuss the choice of the feature map ϕ in Section 8.

Results. Table 1 presents the result of debiasing word embeddings for baseline INLP (Ravfogel et al., 2020) and FaRM. We observe that when compared with INLP, FaRM reduces the accuracy of the network by an absolute margin of 32.4% and achieves a steep increase in MDL. FaRM is able to guard the protected attribute against an attack by a non-linear probing network (near-random accuracy). We also report the rank of the resulting word embedding matrix. The information content of a matrix is captured by its rank (maximal number of linearly independent columns). An increase in rank of the resultant embedding matrix indicates that FaRM is able to retain more information in the representations, in general, compared to INLP.

Visualization. We visualize the t-SNE (Van der Maaten and Hinton, 2008) projections of GloVe embeddings before and after debiasing in Figures 4a and 4b, respectively. Female and male-biased word vectors are represented by **red** and **blue** dots, respectively. The figures clearly

Metric	Method	FastText	BERT
Profession Acc. (↑)	Original	79.9	80.9
	INLP	**76.3**	**77.8**
	FaRM	54.8	55.8
Gender Acc. (↓)	Original	98.9	99.6
	INLP	67.4	94.9
	FaRM	**57.6**	**55.6**
DP (↓)	Original	1.65	1.68
	INLP	1.51	1.50
	FaRM	**0.12**	**0.14**
$\text{Gap}_g^{\text{RMS}}$ (↓)	Original	0.185	0.171
	INLP	0.089	0.096
	FaRM	**0.006**	**0.079**

Table 2: Evaluation results of FaRM on the Biographies dataset. Compared to INLP (Ravfogel et al., 2020), representations from FaRM leak significantly less gender information and achieve better fairness scores.

demonstrate that the gendered vectors are not separable after debiasing. In order to quantify the improvement, we perform k-means clustering with $K = 2$ (one for each gender label). We compute the V-measure (Rosenberg and Hirschberg, 2007)—a measure to quantify the overlap between clusters. V-measure in the original space drops from 99.9% to 0.006% using FaRM (compared to 0.31% using INLP). This indicates that debiased representations from FaRM are more difficult to disentangle. We further analyze the quality of the debiased word embeddings in Section 8.

6.2 Biography Classification

Next, we evaluate FaRM by debiasing text representations in an unconstrained setup and using the representations for fair biography classification.

Setup. We obtain the text representations using two methods: FastText (Joulin et al., 2017) and BERT (Devlin et al., 2019). For FastText, we sum the individual token representations in each biography. For BERT, by retrieving the final layer hidden representation above the `[CLS]` token from a pre-trained BERT$_{\text{base}}$ model. We choose the feature map $\phi(x)$ as a 4-layer neural network with ReLU non-linearity.

Results. Table 2 presents the unconstrained debiasing results of FaRM on this dataset. 'Original' in the table refers to the pre-trained embeddings

from BERT$_{\text{base}}$ or FastText. We observe that FaRM significantly outperforms INLP in fairness metrics—DP (improvement of 92% for FastText and 91% for BERT) and Gap$_{\text{g}}^{\text{RMS}}$ (improvement of 93% for FastText and 18% for BERT). We observe that FaRM achieves near-random gender classification performance (majority baseline: 53.9%) against a non-linear probing attack. FaRM improves upon INLP's gender leakage by an absolute margin of 9.8% and 39.4% for FastText and BERT respectively. However, we observe a substantial drop in the accuracy for identifying professions (target attribute) using the debiased embeddings.[3] This is possibly because in this dataset, gender is highly correlated with the profession and removing gender information results in loss of profession information. Zhao and Gordon (2019) identified this phenomenon by noting the tradeoff between learning fair representations and performing well on target task, when protected and target attributes are correlated. The results in this setup (Table 2) demonstrate this phenomenon. In unconstrained debiasing, we remove information about protected attributes from the representations without taking into account the target task. As a result target task performance suffers from more debiasing.[4] This calls for constrained debiasing for such datasets. In Section 7, we show that FaRM is able to retain target performance while debiasing for this dataset in the constrained setup.

6.3 Controlled Sentiment Classification

Lastly, for the DIAL dataset, we perform unconstrained debiasing in a controlled setting.

Setup. Following the setup of Barrett et al. (2019) and Ravfogel et al. (2020), we control the proportion of protected attributes within a target task class. For example, if target class split $= 80\%$ that means ''happy'' sentiment (target) class contains 80% AAE / 20% SAE, while the ''sad'' class contains 20% AAE / 80% SAE (AAE and SAE are protected class labels mentioned in Section 5.1). We train DeepMoji (Felbo et al., 2017) followed by a 1-layer MLP for sentiment classification. We retrieve representations from the DeepMoji encoder and debias them using FaRM. For debiasing, we choose the feature map $\phi(x)$ to be a

---

[3]Majority baseline for profession classification $\approx$29%.

[4]In our experiments, we found profession accuracy to be high with a shallow feature map or training for earlier epochs, but the gender leakage was significant in these scenarios.

Metric	Method	Split			
		50%	60%	70%	80%
Sentiment Acc. ($\uparrow$)	Original	75.5	75.5	74.4	71.9
	INLP	**75.1**	73.1	**69.2**	**64.5**
	FaRM	74.8	**73.2**	67.3	63.5
Race Acc. ($\downarrow$)	Original	87.7	87.8	87.3	87.4
	INLP	69.5	82.2	80.3	69.9
	FaRM	**54.2**	**69.9**	**69.0**	**52.1**
DP ($\downarrow$)	Original	0.26	0.44	0.63	0.81
	INLP	0.16	0.33	0.30	0.28
	FaRM	**0.09**	**0.10**	**0.17**	**0.22**
Gap$_{\text{g}}^{\text{RMS}}$ ($\downarrow$)	Original	0.15	0.24	0.33	0.41
	INLP	0.12	0.18	0.16	0.16
	FaRM	**0.09**	**0.10**	**0.12**	**0.14**

Table 3: Evaluation results of unconstrained debiasing on the DIAL dataset. We report the performance of the DeepMoji (Original), INLP (Ravfogel et al., 2020), and FaRM representations. We observe that FaRM achieves the best fairness scores in all setups, while maintaining similar performance on sentiment classification task.

7-layer neural network with ReLU non-linearity. After debiasing, we train a non-linear MLP to investigate the quality of debiasing. We evaluate the debiasing performance of FaRM in various stages of label imbalance.

Results. The results of this experiment are reported in Table 3. We see that FaRM is able to achieve the best fairness scores—an improvement in Gap$_{\text{g}}^{\text{RMS}}$ ($\geq$12.5%) and DP ($\geq$21%) across all setups. Considering the accuracy of identifying the protected attribute (race) we can see that FaRM significantly reduces leakage of race information by an absolute margin of 11%–17% across different target class splits. FaRM also achieves similar performance to INLP in sentiment (target attribute) classification. We observe that the fairness score for FaRM deteriorates with an increasing correlation between the protected attribute and the target attribute. In cases where the target and the protected attributes are highly correlated (split $=$ 70% and 80%), we observe a low sentiment classification accuracy (for both INLP and FaRM) compared to the original classifier. This is similar to the observation made for the Biographies dataset and shows that it is difficult to debias information about protected attribute while retaining overall information about

1166

Method	DIAL											
	Sentiment (y)		Race (g)		Fairness		Mention (y)		Race (g)		Fairness	
	F1↑	MDL↓	ΔF1↓	MDL↑	DP↓	$\text{Gap}_g^{\text{RMS}}$↓	F1↑	MDL↓	ΔF1↓	MDL↑	DP↓	$\text{Gap}_g^{\text{RMS}}$↓
BERT$_\text{base}$ (pre-trained)	63.9	300.7	10.9	242.6	0.41	0.20	66.1	290.1	24.6	258.8	0.20	0.10
BERT$_\text{base}$ (fine-tuned)	**76.9**	99.0	18.4	176.2	0.30	0.14	**81.7**	49.1	28.7	199.2	0.06	0.03
AdS	72.9	56.9	5.2	290.6	0.43	0.21	81.1	7.6	21.7	270.3	0.06	0.03
FaRM	73.2	**17.9**	**0.2**	**296.5**	**0.26**	**0.14**	78.8	**3.1**	**0.3**	**324.8**	0.06	0.03

Method	PAN16											
	Mention (y)		Gender (g)		Fairness		Mention (y)		Age (g)		Fairness	
	F1↑	MDL↓	ΔF1↓	MDL↑	DP↓	$\text{Gap}_g^{\text{RMS}}$↓	F1↑	MDL↓	ΔF1↓	MDL↑	DP↓	$\text{Gap}_g^{\text{RMS}}$↓
BERT$_\text{base}$ (pre-trained)	72.3	259.7	7.4	300.5	0.11	0.056	72.8	262.6	6.1	302.0	0.14	0.078
BERT$_\text{base}$ (fine-tuned)	**89.7**	4.0	15.1	267.6	0.04	0.007	**89.3**	4.8	7.4	295.4	0.04	0.006
AdS	89.7	7.6	4.9	**313.9**	0.04	0.007	89.2	6.0	1.1	**315.1**	0.04	**0.004**
FaRM	88.7	**1.7**	**0.0**	312.4	0.04	0.007	88.6	**0.8**	**0.0**	312.6	**0.03**	0.008

Method	BIOGRAPHIES					
	Profession (y)		Gender (g)		Fairness	
	F1↑	MDL↓	ΔF1↓	MDL↑	DP↓	$\text{Gap}_g^{\text{RMS}}$↓
BERT$_\text{base}$ (pre-trained)	74.3	499.9	45.2	27.6	0.43	0.169
BERT$_\text{base}$ (fine-tuned)	99.9	**2.2**	8.3	448.9	0.46	**0.001**
AdS	99.9	3.3	**3.1**	449.5	0.45	0.003
FaRM	99.9	7.6	7.4	**460.3**	**0.42**	0.002

Table 4: Evaluation results for constrained debiasing on DIAL, PAN16, and Biographies. For DIAL and PAN16, we evaluate the approaches for two different configurations of target and proteccted variables, and report the performances in each setting. FaRM outperforms AdS (Basu Roy Chowdhury et al., 2021) in DP metric in all setups, while achieving comparable target task performance.

the target task when the protected attribute is highly correlated with the target attribute. In the constrained setup, we observe FaRM is able to retain target performance (Section 7).

7 Results: Constrained Debiasing

In this section, we present the results of constrained debiasing using FaRM. For all experiments, we use a BERT$_\text{base}$ model as ϕ and a 2-layer neural network with ReLU non-linearity as f (Figure 3).

7.1 Single Attribute Debiasing

In this setup, we focus on debiasing a single protected attribute **g** while retaining information about the target attribute **y**.

Setup. We conduct experiments on 3 datasets: DIAL (Blodgett et al., 2016), PAN16 (Rangel et al., 2016), and Biographies (De-Arteaga et al., 2019). We experiment with different target and protected attribute configurations in DIAL (**y**: Sentiment/Mention, **g**: Race) and PAN16 (**y**: Mention,

g: Gender/Age). For Biographies, we use the same setup as described in Section 6.2. For the protected attribute **g**, we report ΔF1—the difference between F1-score and the majority baseline. We also report fairness metrics: $\text{Gap}_g^{\text{RMS}}$ and Demographic Parity (DP) of the learned classifier. We compare FaRM with the state-of-the-art AdS (Basu Roy Chowdhury et al., 2021), BERT$_\text{base}$ sequence classifier, and pre-trained BERT$_\text{base}$ representations.

Results. Table 4 presents the results of this experiment. We observe that in general, FaRM achieves good fairness performance while maintaining target performance. In particular, it achieves the best DP scores across all setups. In PAN16, FaRM achieves perfect fairness in terms of protected attribute probing accuracy $\Delta F1 = 0$ with comparable performance to AdS in terms of MDL of **g**. In the Biographies dataset, the task accuracy of FaRM is the same as AdS but FaRM outperforms AdS in fairness metrics. We also observe that for this dataset, some baselines performed very well on one (but not both) of the

1167

Setup	PAN16											
	Mention (y)		Age ($\mathbf{g}_1$)		Fairness ($\mathbf{g}_1$)		Gender ($\mathbf{g}_2$)		Fairness ($\mathbf{g}_2$)		Inter. Groups ($\mathbf{g}_1, \mathbf{g}_2$)	
	F1↑	MDL↓	ΔF1↓	MDL↑	DP↓	$\text{Gap}_g^{\text{RMS}}$ ↓	ΔF1↓	MDL↑	DP↓	$\text{Gap}_g^{\text{RMS}}$ ↓	ΔF1↓	MDL↑
BERT$_{\text{base}}$ (fine-tuned)	88.6	6.8	14.9	196.4	0.06	0.009	16.5	192.0	0.04	0.014	20.7	117.2
AdS	**88.6**	**5.5**	2.2	231.5	0.05	0.006	1.6	230.9	0.04	0.017	9.1	118.5
FaRM (N-partition)	87.0	13.4	0.0	234.3	**0.03**	**0.003**	0.0	234.2	0.06	0.025	0.7	**468.0**
FaRM (1-partition)	86.4	15.6	0.0	**234.6**	0.05	0.006	0.0	234.2	**0.02**	**0.009**	**0.0**	467.7

Table 5: Evaluation results for debiasing multiple protected attributes using FaRM. Both configurations of FaRM outperform AdS (Basu Roy Chowdhury et al., 2021) in guarding protected attribute and intersectional group biases.

two fairness metrics, which can be attributed to the inherent tradeoff between them (see Section 5.4). However, FaRM achieves a good balance between the two metrics. Overall, this shows that FaRM is able to robustly remove sensitive information about the protected attribute while achieving good target task performance.

7.2 Multiple Attribute Debiasing

In this setup, we focus on debiasing multiple protected attributes $\mathbf{g}_i$ simultaneously, while retaining information about target attribute $\mathbf{y}$. We evaluate FaRM on the PAN16 dataset with $\mathbf{y}$ as Mention, $\mathbf{g}_1$ as Gender, and $\mathbf{g}_2$ as Age. Subramanian et al. (2021) showed that debiasing a categorical attribute can still reveal information about intersectional groups (e.g., if age (young/old) and gender (male/female) are two categorical protected attributes, then (age = old, gender = male) is an intersectional group). We report the ΔF1/ MDL scores for probing intersectional groups.

Approach. We present two variations of FaRM to remove multiple attributes simultaneously in a constrained setup. Assuming there are N protected attributes, the variations are discussed below:

(a) *N-partition*: In this variation, we compute a membership matrix $\Pi^{\mathbf{g}_i}$ for each protected attribute $\mathbf{g}_i$. We modify Equation 4 as follows:

$$J_c(Z, \mathbf{y}, \Pi^{\mathbf{g}_1}, \ldots, \Pi^{\mathbf{g}_N}) = -\text{CE}(\hat{y}, y)$$
$$+ \lambda \sum_{i=1}^{N} \left[R(Z, \epsilon | \Pi^{\mathbf{g}_i}) - R(Z, \epsilon) \right]$$

(b) *1-partition*: Unlike the previous setup, we can consider each protected attribute $\mathbf{g}_i$ as an independent variable and combine them to form a single protected attribute $\mathcal{G}$. For each input in-

stance, we can represent the ith protected attribute as a one-hot vector $\mathbf{g}_i \in \mathbb{R}^{|\mathbf{g}_i|}$ (where $|\mathbf{g}_i|$ is the dimension of protected attribute $\mathbf{g}_i$). Then the combined vector $\mathcal{G} \in \mathbb{R}^{(|\mathbf{g}_1|+\ldots+|\mathbf{g}_N|)}$ can be obtained by concatenating individual vectors $\mathbf{g}_i$. Since $\mathcal{G}$ is a concatenation of multiple vectors, we normalize $\mathcal{G}$ such that all of its elements sum to 1. Therefore each element of $\mathcal{G}$ is either 0 or $\frac{1}{N}$. We use $\mathcal{G}$ to construct the partition function $\Pi^{\mathcal{G}}$, which captures information about N attributes simultaneously. Each component of $\Pi^{\mathcal{G}}$ satisfies: $\sum_{j=1}^{N} \Pi_j^{\mathcal{G}} = I_{n \times n}$ and $\pi_{ij} \in \{0, \frac{1}{N}\}$. The resultant objective function takes the same form as in Equation 4 with the modified parition function $J_c(Z, Y, \Pi^{\mathcal{G}})$.

Results. We present the results of debiasing multiple attributes in Table 5. We observe that FaRM improves upon AdS' ΔF1-score of age and gender, with N-partition and 1-partition setups performing equally well. The performance on the target task is comparable with AdS, although there is a slight rise in MDL. It is important to note that even though AdS performs decently well in preventing leakage about $\mathbf{g}_1$ and $\mathbf{g}_2$, it still leaks a significant amount of information about the intersectional groups. In both of its configurations, FaRM is able to prevent leakage of intersectional biases while considering the protected attributes independently. This shows that robustly removing information about multiple attributes helps in preventing leakage about intersectional groups as well.

8 Model Analysis

In this section, we present several analysis experiments to evaluate the functioning of FaRM.

Robustness to Label Corruption. We evaluate the robustness of FaRM by randomly
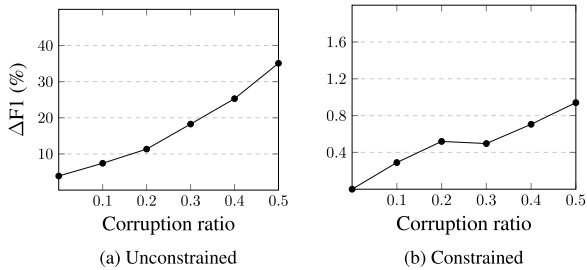
(a) Unconstrained   (b) Constrained

Figure 5: Performance of FaRM with varying fraction of corrupted training set labels in (a) unconstrained and (b) constrained debiasing setups.
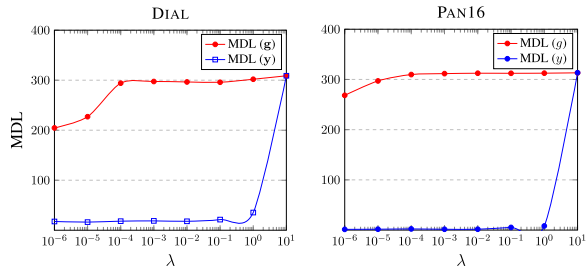

Figure 6: MDL of target ($\mathbf{y}$) and protected ($\mathbf{g}$) attributes with different λ for DIAL and PAN16 datasets.

Method	SimLex-999	WordSim-353	MTurk-771
GloVe	0.374	0.695	0.684
FaRM	0.242	0.503	0.456

Table 6: Word similarity scores before and after debiasing GloVe embeddings using FaRM.

sub-sampling instances from the dataset and modifying the protected attribute label. In Figure 5a, we report the protected attribute leakage (ΔF1 score) from the debiased word embeddings with varying fractions of training set label corruption. We observe that FaRM's performance degrades with an increase in label corruption. This is expected as, at high corruption ratios, most of the protected attribute labels are wrong, resulting in poor performance.

In the constrained setup (Figure 5b), we observe that FaRM is able to debias protected attribute information (y-axis scale in Figure 5b and 5a are different) even at high corruption ratios. We believe this enhanced performance (compared to unconstrained setup) is due to the additional supervision in the form of target loss, which enables FaRM to learn robust representations even with corrupted protected attribute labels.

Sensitivity to λ. We measure the sensitivity of FaRM's performance w.r.t. λ (Equation 4) in the constrained setup. In Figure 6, we show the MDL of the target attribute $\mathbf{y}$ (in **blue**) and protected attribute $\mathbf{g}$ (in **red**) for DIAL and PAN16 for different λ. We observe that when $10^{-4} \leq \lambda \leq 1$, the performance of FaRM does not change much. For $\lambda = 10$, MDL for $\mathbf{y}$ is quite

large, showcasing that the model does not converge on the target task. This is expected as the regularization term (Equation 4) is much larger than $\mathrm{CE}(\hat{y}, y)$ term, and boosting it further with $\lambda = 10$ makes it difficult for the target task loss to converge. Similarly, when $\lambda \leq 10^{-5}$, the regularization term is much smaller compared to $\mathrm{CE}(\hat{y}, y)$, and there is a substantial drop in MDL for $\mathbf{g}$. However, we show that FaRM achieves good performance over a broad spectrum of λ. Therefore, reproducing the desired results does not require extensive hyperparameter tuning.

Probing Word Embeddings. A limitation of using FaRM for debiasing word embeddings is that distances in the original embedding space are not preserved. The Mazur–Ulam theorem (Fleming and Jamison, 2003) states that isometry for a mapping $\phi : V \to W$ is preserved only if the function ϕ is affine. FaRM uses a non-linear feature map $\phi(x)$. Therefore, distances cannot be preserved. A linear map $\phi(x)$ is also not ideal because it does not guard protected attributes against an attack by a non-linear probing network. We investigate the utility of debiased embeddings by performing the following experiments:

(a) *Word Similarity Evaluation*: In this experiment, we evaluate the debiased embeddings on the following datasets: SimLex-999 (Hill et al., 2015), WordSim-353 (Agirre et al., 2009), and MTurk-771 (Halawi et al., 2012). In Table 6, we report the Spearman correlation between the gold similarity scores of word pairs and the cosine similarity scores obtained before (top row) and after (bottom row) debiasing GloVe embeddings. We observe a significant drop in correlation with gold scores, which is expected since debiasing is removing some information from the embeddings. In spite of the drop, there is a reasonable correlation with the gold scores indicating that FaRM is able to retain a significant degree of semantic information.

(b) *Part-of-speech Tagging*: We evaluate debiased embeddings for detecting POS tags in a
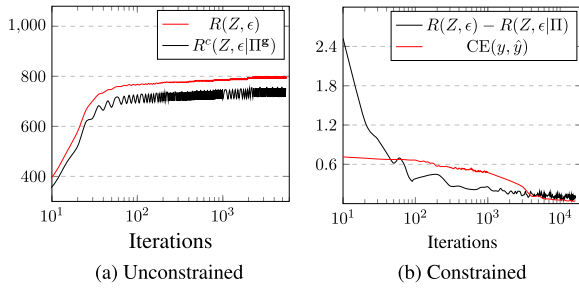
(a) Unconstrained   (b) Constrained

Figure 7: Loss evolution in the unconstained setup (left) where both terms – $R(Z,\epsilon)$ (**red**) and $R^c(Z,\epsilon|\Pi^{\mathbf{g}})$ (**black**) start increasing simultaneously. In the constrained setup (right) with $\lambda = 0.01$ – bias loss (**black**) starts converging earlier than the target loss (**red**).

sentence using the Universal tagset (Petrov et al., 2012). GloVe embeddings achieve an F1-score of 95.2% and FaRM achieves an F1-score of 93.0% on this task. This shows FaRM's debiased embeddings still possess a significant amount of morphological information about the language.

(c) *Sentiment Classification*: We perform sentiment classification using word embeddings on the IMDb movies dataset (Maas et al., 2011). GloVe embeddings achieve an accuracy of 80.9%, while debiased embeddings achieve an accuracy of 74.6%. The drop in this task is slightly more compared to POS tagging, but FaRM is still able to achieve reasonable performance on this task.

These experiments showcase that even though exact distances aren't preserved using FaRM, the debiased embeddings still retain relevant information useful in downstream tasks.

Evolution of Loss Components. We evaluate how FaRM's loss components evolve during training. In the unconstrained setup for GloVe debiasing, we evaluate how the evolution of components—$R(Z,\epsilon)$ (in **red**) and $R^c(Z,\epsilon|\Pi^{\mathbf{g}})$ (in **black**). In Figure 7a, we observe that both loss terms start increasing simultaneously, with their difference remaining constant in the final iterations. Next in the constrained setup, the evolution of target loss $CE(\hat{y}, y)$ and bias loss $R(Z,\epsilon) - R^c(Z,\epsilon|\Pi^{\mathbf{g}})$ for DIAL dataset are shown in Figure 7b. We observe that the bias term converges first followed by the target loss. This is expected as the magnitude of rate-distortion loss is larger than target loss, which forces the model to minimize it first.

Limitations. A limitation of FaRM is that we lack a principled feature map $\phi(x)$ selection approach. In the unconstrained setup, we relied on empirical observations and found that a 4-layer ReLU network sufficed for GloVe and Biographies, while a 7-layer network was required for DIAL. For the constrained setup, BERT$_{\text{base}}$ proved to be expressive enough to perform debiasing in all setups. Future works can explore white-box network architectures (Chan et al., 2022) for debiasing.

9 Conclusion

We proposed **Fa**irness-aware **R**ate **M**aximization (FaRM), a novel debiasing technique based on the principle of rate-distortion maximization. FaRM is effective in removing protected information from representations in both unconstrained and constrained debiasing setups. Empirical evaluations show that FaRM outperforms prior works in debiasing representations by a large margin on several datasets. Extensive analysis showcase that FaRM is sample efficient, and robust to label corruptions and minor hyperparameter changes. Future works can focus on leveraging FaRM for achieving fairness in complex tasks like language generation.

10 Ethical Considerations

In this work, we present FaRM—a robust representation learning framework to selectively remove protected information. FaRM is developed with an intent to enable development of fair learning systems. However, FaRM can be misused to remove salient features from representations and perform classification by leveraging demographic information. Debiasing using FaRM is only evaluated on datasets with binary protected attribute variables. This may not be ideal while removing protected information about gender, which can extend beyond binary categories. Currently, we lack datasets with fine-grained gender annotation. It is important to collect data and develop techniques, that would benefit everyone in our community.

References

Eneko Agirre, Enrique Alfonseca, Keith Hall, Jana Kravalova, Marius Paşca, and Aitor Soroa. 2009. A study on similarity and relatedness

using distributional and WordNet-based approaches. In *Proceedings of Human Language Technologies: The 2009 Annual Conference of the North American Chapter of the Association for Computational Linguistics*, pages 19–27, Boulder, Colorado. Association for Computational Linguistics. https://doi.org/10.3115/1620754.1620758

Jimmy Lei Ba, Jamie Ryan Kiros, and Geoffrey E. Hinton. 2016. Layer normalization. *arXiv preprint arXiv:1607.06450*

Maria Barrett, Yova Kementchedjhieva, Yanai Elazar, Desmond Elliott, and Anders Søgaard. 2019. Adversarial removal of demographic attributes revisited. In *Proceedings of the 2019 Conference on Empirical Methods in Natural Language Processing and the 9th International Joint Conference on Natural Language Processing (EMNLP-IJCNLP)*, pages 6330–6335, Hong Kong, China. Association for Computational Linguistics. https://doi.org/10.18653/v1/D19-1662

Kanadpriya Basu, Treena Basu, Ron Buckmire, and Nishu Lal. 2019. Predictive models of student college commitment decisions using machine learning. *Data*, 4(2):65. https://doi.org/10.3390/data4020065

Somnath Basu Roy Chowdhury, Sayan Ghosh, Yiyuan Li, Junier Oliva, Shashank Srivastava, and Snigdha Chaturvedi. 2021. Adversarial scrubbing of demographic information for text classification. In *Proceedings of the 2021 Conference on Empirical Methods in Natural Language Processing*, pages 550–562, Online and Punta Cana, Dominican Republic. Association for Computational Linguistics. https://doi.org/10.18653/v1/2021.emnlp-main.43

Peter J. Bickel, Eugene A. Hammel, and J. William O'Connell. 1975. Sex bias in graduate admissions: Data from berkeley: Measuring bias is harder than is usually assumed, and the evidence is sometimes contrary to expectation. *Science*, 187(4175):398–404. https://doi.org/10.1126/science.187.4175.398, PubMed: 17835295

Su Lin Blodgett, Lisa Green, and Brendan O'Connor. 2016. Demographic dialectal variation in social media: A case study of African-American English. In *Proceedings of the 2016 Conference on Empirical Methods in Natural Language Processing*, pages 1119–1130, Austin, Texas. Association for Computational Linguistics. https://doi.org/10.18653/v1/D16-1120

Tolga Bolukbasi, Kai-Wei Chang, James Y. Zou, Venkatesh Saligrama, and Adam Tauman Kalai. 2016. Man is to computer programmer as woman is to homemaker? debiasing word embeddings. In *Advances in Neural Information Processing Systems 29: Annual Conference on Neural Information Processing Systems 2016, December 5–10, 2016, Barcelona, Spain*, pages 4349–4357.

John D. Burger, John Henderson, George Kim, and Guido Zarrella. 2011. Discriminating gender on Twitter. In *Proceedings of the 2011 Conference on Empirical Methods in Natural Language Processing*, pages 1301–1309. Edinburgh, Scotland, UK. Association for Computational Linguistics.

Kwan Ho Ryan Chan, Yaodong Yu, Chong You, Haozhi Qi, John Wright, and Yi Ma. 2022. Redunet: A white-box deep network from the principle of maximizing rate reduction. *Journal of Machine Learning Research*, 23(114):1–103.

Thomas M. Cover. 1999. *Elements of Information Theory*. John Wiley & Sons.

Maria De-Arteaga, Alexey Romanov, Hanna Wallach, Jennifer Chayes, Christian Borgs, Alexandra Chouldechova, Sahin Geyik, Krishnaram Kenthapadi, and Adam Tauman Kalai. 2019. Bias in bios: A case study of semantic representation bias in a high-stakes setting. In *proceedings of the Conference on Fairness, Accountability, and Transparency*, pages 120–128. https://doi.org/10.1145/3287560.3287572

Sunipa Dev, Tao Li, Jeff M. Phillips, and Vivek Srikumar. 2021. OSCaR: Orthogonal subspace correction and rectification of biases in word embeddings. In *Proceedings of the 2021 Conference on Empirical Methods in Natural Language Processing*, pages 5034–5050, Online and Punta Cana, Dominican Republic. Association for Computational Linguistics. https://doi.org/10.18653/v1/2021.emnlp-main.411

Jacob Devlin, Ming-Wei Chang, Kenton Lee, and Kristina Toutanova. 2019. BERT: Pre-training of deep bidirectional transformers for language understanding. In *Proceedings of the 2019 Conference of the North American Chapter of the Association for Computational Linguistics: Human Language Technologies, Volume 1 (Long and Short Papers)*, pages 4171–4186, Minneapolis, Minnesota. Association for Computational Linguistics.

Yanai Elazar and Yoav Goldberg. 2018. Adversarial removal of demographic attributes from text data. In *Proceedings of the 2018 Conference on Empirical Methods in Natural Language Processing*, pages 11–21, Brussels, Belgium. Association for Computational Linguistics. https://doi.org/10.18653/v1/D18-1002

Yanai Elazar, Shauli Ravfogel, Alon Jacovi, and Yoav Goldberg. 2021. Amnesic probing: Behavioral explanation with amnesic counterfactuals. *Transactions of the Association for Computational Linguistics*, 9:160–175. https://doi.org/10.1162/tacl_a_00359

Bjarke Felbo, Alan Mislove, Anders Søgaard, Iyad Rahwan, and Sune Lehmann. 2017. Using millions of emoji occurrences to learn any-domain representations for detecting sentiment, emotion and sarcasm. In *Proceedings of the 2017 Conference on Empirical Methods in Natural Language Processing*, pages 1615–1625, Copenhagen, Denmark. Association for Computational Linguistics. https://doi.org/10.18653/v1/D17-1169

Richard J. Fleming and James E. Jamison. 2003. *Function Spaces*. Chapman & Hall/CRC.

Omar Ghailan, Hoda MO Mokhtar, and Osman Hegazy. 2016. Improving credit scorecard modeling through applying text analysis. *Institutions*, 7(4). https://doi.org/10.14569/IJACSA.2016.070467

Ian Goodfellow, Jean Pouget-Abadie, Mehdi Mirza, Bing Xu, David Warde-Farley, Sherjil Ozair, Aaron Courville, and Yoshua Bengio. 2014. Generative adversarial nets. In *Advances in Neural Information Processing Systems*, volume 27. Curran Associates, Inc.

Guy Halawi, Gideon Dror, Evgeniy Gabrilovich, and Yehuda Koren. 2012. Large-scale learning of word relatedness with constraints. In *The 18th ACM SIGKDD International Conference on Knowledge Discovery and Data Mining, KDD '12, Beijing, China, August 12–16, 2012*, pages 1406–1414. ACM. https://doi.org/10.1145/2339530.2339751

Felix Hill, Roi Reichart, and Anna Korhonen. 2015. SimLex-999: Evaluating semantic models with (genuine) similarity estimation. *Computational Linguistics*, 41(4):665–695. https://doi.org/10.1162/COLI_a_00237

Armand Joulin, Edouard Grave, Piotr Bojanowski, and Tomas Mikolov. 2017. Bag of tricks for efficient text classification. In *Proceedings of the 15th Conference of the European Chapter of the Association for Computational Linguistics: Volume 2, Short Papers*, pages 427–431, Valencia, Spain. Association for Computational Linguistics. https://doi.org/10.18653/v1/E17-2068

Moshe Koppel, Shlomo Argamon, and Anat Rachel Shimoni. 2002. Automatically categorizing written texts by author gender. *Literary and Linguistic Computing*, 17(4):401–412. https://doi.org/10.1093/llc/17.4.401

Yitong Li, Timothy Baldwin, and Trevor Cohn. 2018. Towards robust and privacy-preserving text representations. In *Proceedings of the 56th Annual Meeting of the Association for Computational Linguistics (Volume 2: Short Papers)*, pages 25–30, Melbourne, Australia. Association for Computational Linguistics.

Ilya Loshchilov and Frank Hutter. 2019. Decoupled weight decay regularization. In *7th International Conference on Learning Representations, ICLR 2019, New Orleans, LA, USA, May 6–9, 2019*. OpenReview.net.

Yi Ma, Harm Derksen, Wei Hong, and John Wright. 2007. Segmentation of multivariate mixed data via lossy data coding and compression. *IEEE Transactions on Pattern Analysis and Machine Intelligence*, 29(9):1546–1562. https://doi.org/10.1109/TPAMI.2007.1085, PubMed: 17627043

Andrew L. Maas, Raymond E. Daly, Peter T. Pham, Dan Huang, Andrew Y. Ng, and Christopher Potts. 2011. Learning word vectors for sentiment analysis. In *Proceedings of*

the 49th Annual Meeting of the Association for Computational Linguistics: Human Language Technologies, pages 142–150, Portland, Oregon, USA. Association for Computational Linguistics.

Laurens Van der Maaten and Geoffrey Hinton. 2008. Visualizing data using t-sne. *Journal of Machine Learning Research*, 9(11).

Jan Macdonald, Stephan Wäldchen, Sascha Hauch, and Gitta Kutyniok. 2019. A rate-distortion framework for explaining neural network decisions. *ArXiv preprint*, abs/1905.11092.

Ninareh Mehrabi, Fred Morstatter, Nripsuta Saxena, Kristina Lerman, and Aram Galstyan. 2021. A survey on bias and fairness in machine learning. *ACM Computing Surveys*, 54(6). https://doi.org/10.1145/3457607

Dong Nguyen, Rilana Gravel, Dolf Trieschnigg, and Theo Meder. 2013. ''How old do you think i am?'' A study of language and age in Twitter. In *Proceedings of the International AAAI Conference on Web and Social Media*, volume 7.

Fabian Pedregosa, Gaël Varoquaux, Alexandre Gramfort, Vincent Michel, Bertrand Thirion, Olivier Grisel, Mathieu Blondel, Peter Prettenhofer, Ron Weiss, Vincent Dubourg, and Jake Vanderplas, Alexandre Passos, David Cournapeau, Matthieu Brucher, Matthieu Perrot, and Édouard Duchesnay. 2011. Scikit-learn: Machine learning in Python. *Journal of Machine Learning Research*, 12:2825–2830.

Slav Petrov, Dipanjan Das, and Ryan McDonald. 2012. A universal part-of-speech tagset. In *Proceedings of the Eighth International Conference on Language Resources and Evaluation (LREC'12)*, pages 2089–2096, Istanbul, Turkey. European Language Resources Association (ELRA).

Francisco Rangel, Paolo Rosso, Ben Verhoeven, Walter Daelemans, Martin Potthast, and Benno Stein. 2016. Overview of the 4th author profiling task at pan 2016: Cross-genre evaluations. *Working Notes Papers of the CLEF*, 2016:750–784.

Shauli Ravfogel, Yanai Elazar, Hila Gonen, Michael Twiton, and Yoav Goldberg. 2020. Null it out: Guarding protected attributes by iterative nullspace projection. In *Proceedings of the 58th Annual Meeting of the Association for Computational Linguistics*, pages 7237–7256, Online. Association for Computational Linguistics. https://doi.org/10.18653/v1/2020.acl-main.647

Alexey Romanov, Maria De-Arteaga, Hanna Wallach, Jennifer Chayes, Christian Borgs, Alexandra Chouldechova, Sahin Geyik, Krishnaram Kenthapadi, Anna Rumshisky, and Adam Kalai. 2019. What's in a name? Reducing bias in bios without access to protected attributes. In *Proceedings of the 2019 Conference of the North American Chapter of the Association for Computational Linguistics: Human Language Technologies, Volume 1 (Long and Short Papers)*, pages 4187–4195, Minneapolis, Minnesota. Association for Computational Linguistics. https://doi.org/10.18653/v1/N19-1424

Andrew Rosenberg and Julia Hirschberg. 2007. V-measure: A conditional entropy-based external cluster evaluation measure. In *Proceedings of the 2007 Joint Conference on Empirical Methods in Natural Language Processing and Computational Natural Language Learning (EMNLP-CoNLL)*, pages 410–420, Prague, Czech Republic. Association for Computational Linguistics.

Shivashankar Subramanian, Xudong Han, Timothy Baldwin, Trevor Cohn, and Lea Frermann. 2021. Evaluating debiasing techniques for intersectional biases. In *Proceedings of the 2021 Conference on Empirical Methods in Natural Language Processing*, pages 2492–2498, Online and Punta Cana, Dominican Republic. Association for Computational Linguistics. https://doi.org/10.18653/v1/2021.emnlp-main.193

Ben Verhoeven and Walter Daelemans. 2014. CLiPS stylometry investigation (CSI) corpus: A Dutch corpus for the detection of age, gender, personality, sentiment and deception in text. In *Proceedings of the Ninth International Conference on Language Resources and Evaluation (LREC'14)*, pages 3081–3085, Reykjavik, Iceland. European Language Resources Association (ELRA).

Ben Verhoeven, Walter Daelemans, and Barbara Plank. 2016. TwiSty: A multilingual Twitter stylometry corpus for gender and personality profiling. In *Proceedings of the Tenth International Conference on Language Resources and Evaluation (LREC'16)*, pages 1632–1637, Portorož, Slovenia. European Language Resources Association (ELRA).

Elena Voita and Ivan Titov. 2020. Information-theoretic probing with minimum description length. In *Proceedings of the 2020 Conference on Empirical Methods in Natural Language Processing (EMNLP)*, pages 183–196, Online. Association for Computational Linguistics. `https://doi.org/10.18653/v1/2020.emnlp-main.14`

Edson R. D. Weren, Anderson U. Kauer, Lucas Mizusaki, Viviane P. Moreira, J. Palazzo, M. de Oliveira, and Leandro K. Wives. 2014. Examining multiple features for author profiling. *Journal of Information and Data Management*, 5(3):266–266.

Qizhe Xie, Zihang Dai, Yulun Du, Eduard H. Hovy, and Graham Neubig. 2017. Controllable invariance through adversarial feature learning. In *Advances in Neural Information Processing Systems 30: Annual Conference on Neural Information Processing Systems 2017, December 4–9, 2017, Long Beach, CA, USA*, pages 585–596.

Yaodong Yu, Kwan Ho Ryan Chan, Chong You, Chaobing Song, and Yi Ma. 2020. Learning diverse and discriminative representations via the principle of maximal coding rate reduction. In *Advances in Neural Information Processing Systems*, volume 33, pages 9422–9434. Curran Associates, Inc.

Richard S. Zemel, Yu Wu, Kevin Swersky, Toniann Pitassi, and Cynthia Dwork. 2013. Learning fair representations. In *Proceedings of the 30th International Conference on Machine Learning, ICML 2013, Atlanta, GA, USA, 16–21 June 2013*, volume 28 of *JMLR Workshop and Conference Proceedings*, pages 325–333. JMLR.org.

Brian Hu Zhang, Blake Lemoine, and Margaret Mitchell. 2018. Mitigating unwanted biases with adversarial learning. In *Proceedings of the 2018 AAAI/ACM Conference on AI, Ethics, and Society*, pages 335–340. `https://doi.org/10.1145/3278721.3278779`

Han Zhao and Geoffrey J. Gordon. 2019. Inherent tradeoffs in learning fair representations. In *Advances in Neural Information Processing Systems 32: Annual Conference on Neural Information Processing Systems 2019, NeurIPS 2019, December 8–14, 2019, Vancouver, BC, Canada*, pages 15649–15659.

Jieyu Zhao, Yichao Zhou, Zeyu Li, Wei Wang, and Kai-Wei Chang. 2018. Learning gender-neutral word embeddings. In *Proceedings of the 2018 Conference on Empirical Methods in Natural Language Processing*, pages 4847–4853, Brussels, Belgium. Association for Computational Linguistics. `https://doi.org/10.18653/v1/D18-1521`